ACCELERATION-INSENSITIVE FULLY-DECOUPLED TUNING FORK (FDTF) MEMS VIBRATORY GYROSCOPE WITH 1°/HR BIAS INSTABILITY

Feng-Yu Lee[1], Kai-Chih Liang[1], Emerson Cheng[1,2], Sheng-Shian Li[1,3] and Weileun Fang[1,3]
[1]Power Mechanical Engineering Department, National Tsing-Hua University, Hsinchu, Taiwan
[2]Taiwan Semiconductor Manufacturing Company Ltd., Hsinchu Science Park, Hsinchu, Taiwan
[3]Institute of NanoEngineering and MicroSystems, National Tsing-Hua University, Hsinchu, Taiwan

ABSTRACT

This study presents the design and implementation of a single-axis MEMS vibratory gyroscope with reduced coupling error and enhanced vibration resistance. Features of this study are (1) exploiting the fully-decoupled mechanism to minimize the coupling error between the operating modes; (2) introducing the tuning fork architecture combined with specific coupler designs to enhance the vibration resistance; (3) a compact structural design with small footprint (2mm ×2mm). Measurement results show a reduced coupling error signal of near 126°/s, and the acceleration sensitivity is below 1.5°/s/g. Moreover, the angular rate sensitivity is 1.25mV/°/s and the non-linearity is 0.68% within ±300°/s. Contributed to the reduction of the coupling error and external vibration interference, the FDTF gyroscope achieved a bias instability of 1°/hr and the ARW of 7.2°/hr/°Hz.

INTRODUCTION

The applications of MEMS gyroscopes are gradually expanding from automotive to consumer and personal electronics. Moreover, with the potential for high-end applications, like INS, IMUs and IoTs products [1], the demand for high performance MEMS gyroscopes is also increased. Thus, to meet the requirements, improving the noise level and the longtime operation stability are two critical design considerations.

For the MEMS Coriolis vibratory gyroscopes (CVGs), one of the major design issues is the coupling error due to the manufacturing tolerances. Any imbalances of the springs or the electrodes would yield a large coupling motion between the operating modes, resulting in a large error signal [2]. Most of such error signal can be compensated by phase-sensitive demodulation techniques. However, even very small phase error could still result in considerable offset variations at the output of the gyroscope. Various approaches have been reported to alleviate this problem. The earlier approach is the laser trimming [3], which is time-consuming and relatively expensive. The electronic cancellation techniques by injecting an electrical signal to the sense-mode or applying a specific dc potential to the mechanical electrodes have been reported in [4-5]. However, these approaches need precise electronic control and have a smaller compensation range. Thus, to have a better reduction of the coupling motion, some literatures have demonstrated the decoupled structural designs [6-7]. These designs do not require any additional electronics and can greatly reduce the coupling motion. However, the complicated structure and large footprint could limit the applications.

Another design issue for MEMS CVGs is the interference from external vibrations. This common-mode, acceleration-induced force is several orders of magnitude larger than the rate-induced Coriolis force. Therefore, extracting the correct rate signal or suppressing the acceleration-induced motion is very critical to most CVGs design. Vibrating ring (degenerate) gyroscopes [8] leverage the symmetric, flexure modes, and much higher operating frequencies to minimize the acceleration signal. However, narrow bandwidth and small sensing gap remain some considerable issues. For the ease of control circuit and structural design, the dual-masses (tuning fork) architecture is commonly used in nondegenerate CVGs [9-10] to eliminate the common-mode interferences with the differential sensing scheme.

In order to improve both the coupling error and the vibration resistance, a fully-decoupled tuning fork (FDTF) gyroscope had been reported [11]. The preliminary tests show this design can achieve lower coupling error (~500°/s) and the acceleration sensitivity is below 120°/s/g. Furthermore, this study presents a modified design of the existing system, including the sensing circuit and the measurement setup, to reduce the parasitic effect and enhance the sensitivity. As a result, the gyroscope performance can be further improved.

DESIGN CONCEPT

Fig.1 shows the schematic of the proposed gyro structure, which consists of dual drive-masses (M_{d1}, M_{d2}), dual coupling-masses (M_{c1}, M_{c2}) and dual sense-masses (M_{s1}, M_{s2}). These masses are connected to each other by

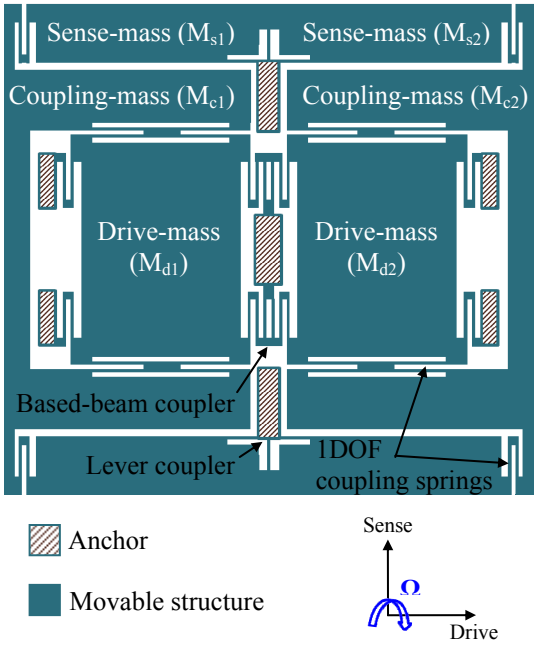

Figure 1: The structural schematic of a FDTF gyroscope.

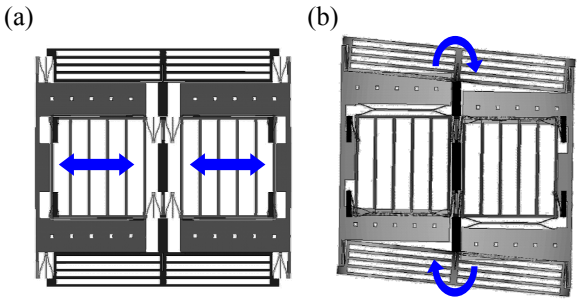

Figure 2: Operating modes of the FDTF gyroscope. (a) drive-mode, (b) sense-mode.

several 1DOF coupling springs to form two decoupled gyroscope systems (with subscript 1, 2). Moreover, the lever coupler and based-beam coupler are utilized to connect the sense-masses and drive-masses respectively, resulting in the mechanical couplings between the two gyroscope systems (tuning fork architecture). Thus, as the gyroscope starts operating, both the drive-masses and the coupling-masses would be driven into an anti-phase motion, but the sense-masses remain stationary due to the 1DOF coupling springs. Such design refers to a "drive-decoupled" operation. Furthermore, as a (yaw-axis) angular rate exerts on the gyroscope, the Coriolis force would be introduced on the coupling-masses, and forces them to move along the sense direction. Due to the opposite driving velocity of the coupling-masses and the lever coupler design, the sense-masses would be driven into a seesaw motion by the coupling-masses. Likewise, due to the 1DOF coupling springs, the motion of the coupling-masses along the sense direction would not influence the driving motion of the drive-masses. This refers to a "sense-decoupled" operation. Thus, this structural design combines the tuning fork architecture with the drive-decoupled and sense-decoupled operation, resulting in a "FDTF" gyroscope. Fig.2 depicts the simulation results of the drive-mode and the sense-mode of the FDTF gyro respectively, proving the decoupled motion between the operating modes. As a result, this design can minimize the gyroscope coupling error and, with a proper sensing scheme, reject the common-mode interferences.

FABRICATION AND RESULTS

This device is realized using TSMC bulk MEMS process [12], which is established for sensors implementation and integration. Features of this process include thick single crystal silicon (~30μm) as the MEMS structure and poly-silicon plugs and interconnections for electrical routing, as in Fig.3. A wafer level bonding process is also employed to provide a hermetically sealed cavity inside the device. Vacuum-sealing capability is also available for this process (below several torr), and thus, this platform is suitable for the gyroscope development.

Micrographs in Fig.4(a-d) show the close view of the components on a decap gyro chip. As depicted in Fig.4(a), the gyroscope footprint is 2mm×2mm. The lever coupler, as shown in Fig.4(b), is consisting of 3 clamped-clamped beams. These beams are located at the same anchor, but are separated to each other by 90°. This arrangement ensures strong resistance to the linear motion of the sense-masses,

Figure 3: Cross-section of the TSMC bulk MEMS process.

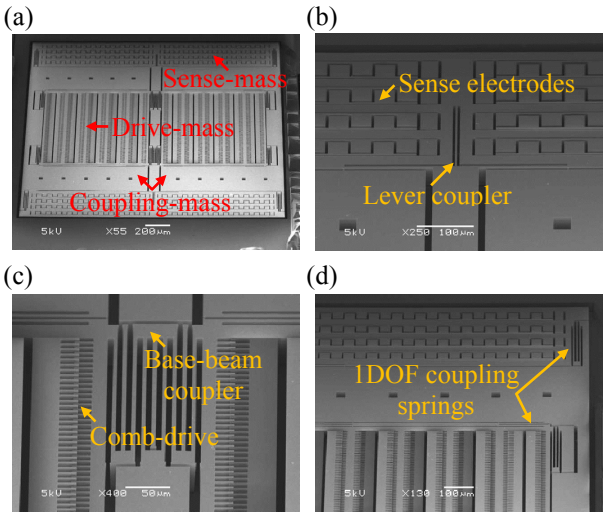

Figure 4: SEM micrographs of a decap FDTF gyro chip.

yet the rotation around the anchor remains available. Thus, the sense-masses are capable of sensing the Coriolis force (by seesaw motion) and reject the acceleration-induced force. Fig.4(c) shows the based-beam coupler, which consists of two pairs of folded springs. These springs are connected to the anchor through a thick truss. Thus, as the drive-masses are driven into an anti-phase motion, the truss would remain stationary and reduce the energy loss through the anchor. Moreover, the coupling-masses are connected to the drive-masses and sense-masses by the orthogonal arranged 1DOF coupling springs, as shown in Fig.4(d). These coupling springs are designed to be flexible in only one direction. Thus, the motion of the drive-masses and the sense-masses is independent to each other, which reduces the coupling error.

As shown in Fig.5(a), the total chip size is 4mm ×4mm, including the FDTF gyro (2mm×2mm) and testing structures. The gyro chip is further wire-bonded on a ceramic DIP for measurement purpose. Fig.5(b) shows the DIP combined with a customized circuit board, which is implemented on the commercial rate table (Acutronic AC1120S). Several co-axial cables are utilized to pass the electrical signals through the rate table.

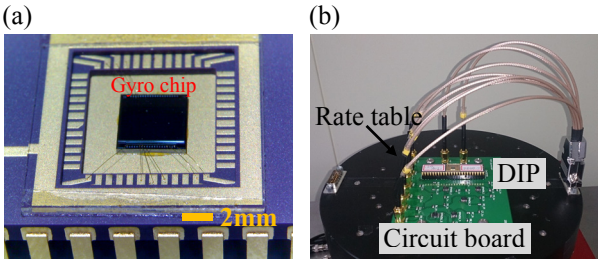

Figure 5: A fabricated FDTF gyro chip (a) wire-bonded on a DIP; (b) integrated with a PCB circuit board.

MEASUREMENT AND DISCUSSION

Fig.6 shows the angular rate measurement setup. The measurement instruments, including the power and DC/AC sources, are directly connected to the rate table. The readout signal of the circuit board is picked up by a DAQ card and processed by NI SignalExpress software for real-time signal extraction and noise analysis. The rotation motion of the rate table is controlled by the computer to offer the constant speed and reversed-direction operations for gyro characterization.

For the proposed gyro design, the resonant frequency of the drive-mode is about 6.1kHz and the sense-mode is about 6.3kHz. The quality factor of the drive-mode and sense-mode is 250 and 85 respectively. Furthermore, Fig.7 shows the gyro output w.r.t. different angular rate input. With a 6V bias and 2V sinusoidal driving signal, the angular rate sensitivity of a FDTF gyro is 1.25mV/°/s, and the non-linearity is 0.68% within ±300°/s measurement range. The angular rate sensitivity is 70 times larger than the previous work (17.7μV/°/s) [11] due to the improved readout circuit design.

The coupling error of the FDTF gyro is extracted using an alternative angular rate input, as shown in Fig.8. The central peak indicates the coupling-motion-equivalent angular rate. The side bands are due to the square-wave angular rate input. Thus, from the measurement, the coupling error of a FDTF gyro is about 126°/s, which is a quarter of the previous work (~500°/s) [11]. This is attributed to the reduction of the electrical feed-through utilizing a refined measurement setup.

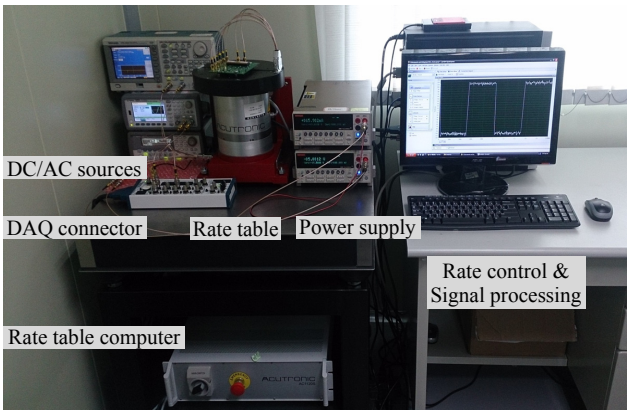

Figure 6: Angular rate measurement setup.

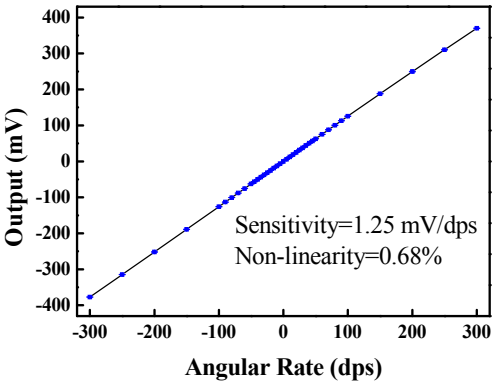

Figure 7: Angular rate sensitivity of a FDTF gyroscope.

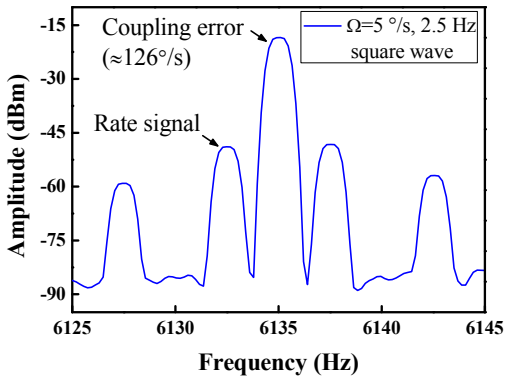

Figure 8: Coupling error measurement of a FDTF gyro under an alternative angular rate input.

Besides the coupling error reduction, the other design target of this study is to enhance the vibration resistance. Such characteristic can be evaluated by the acceleration testing setup shown in Fig.9(a). A commercial shaker (B&K Corporation, LDS V406) is utilized to generate a periodic excitation to the gyro chip with frequency of 30Hz and amplitude of ±2g. The excitation is monitored by a commercial accelerometer. Measurement results depicted in Fig.9(b) show the gyro output w.r.t. different excitation directions. It indicates the acceleration sensitivity of the FDTF gyro is 1.5°/s/g in drive direction, 1.1°/s/g in sense direction, and 0.6°/s/g in out-of-plane direction, proving the higher vibration resistance using the tuning fork architecture and specific coupler designs. Note that the amplitude variation of the vibration signal in Fig.9(b) is due to the oscillation of the connection cables.

(a)

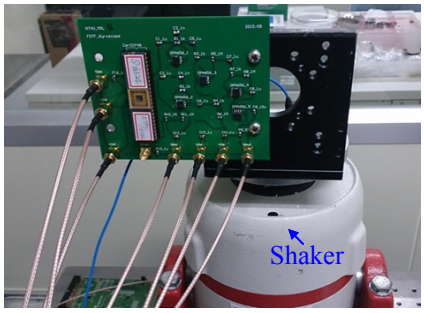

(b)

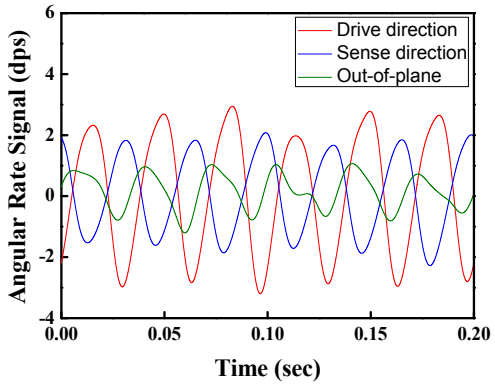

Figure 9: Acceleration sensitivity a FDTF gyro under external vibrations. (a) measurement setup; (b) applying a 30 Hz, ±2g acceleration along different directions.

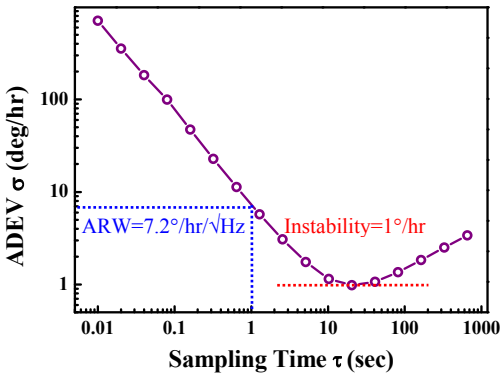

Figure 10: Allan variance analysis of a FDTF gyro.

As the FDTF gyro minimizes both the coupling error signal and external vibration interference, it also implies the possibility of this device for lower noise level and better longtime stability. Fig.10 shows the Allan variance analysis of a FDTF gyro using the overlapped sampling technique. It indicates the bias instability of 1°/hr and the ARW of 7.2°/hr/√Hz.

CONCLUSION

This study demonstrates a MEMS vibratory gyroscope, which integrates the fully-decoupled mechanism and the tuning fork architecture (i.e. a FDTF gyro), to reduce both the coupling error and vibration interference. Attributed to the specific coupling spring design, the motion of the drive-masses and sense-masses is independent, resulting in a minimized coupling motion (~126°/s). The lever coupler combined with the anti-phase drive/sense motion increases the vibration resistance, and the acceleration sensitivity is below 1.5°/s/g. Moreover, the FDTF gyro achieves bias instability of 1°/hr and ARW of 7.2°/hr/√Hz, showing the possibility for future high-end applications.

ACKNOWLEDGEMENT

This study was partially supported by the Ministry of Science and Technology of Taiwan (grant number MOST 104-2221-E-007-016-MY3) and the National Applied Research Laboratories of Taiwan (grant number NARL-IOT-104-001). The authors would also like to appreciate the Taiwan Semiconductor Manufacturing Company Ltd (TSMC) for manufacturing service and Center for Nanotechnology, Materials Science and Microsystems (CNMM) of National Tsing Hua University and the Taiwan National Nano Device Laboratory (NDL) for the fabrication facility support.

REFERRENCE

[1] B. R. Johnson, E. Cabuz, H. B. French, and R. Supino, "Development of a MEMS gyroscope for northfinding applications," *PLANS*, Indian Wells, CA, May, 2010, pp. 168–170.

[2] E. Tatar, S. E. Alper and T. Akin, "Quadrature-Error Compensation and Corresponding Effects on the Performance of Fully Decoupled MEMS Gyroscopes," *Journal of Microelectromechanical Systems*, Vol. 21, pp. 656-667, 2012.

[3] M. Saukoski, L. Aaltonen, and K. A. I. Halonen, "Zero-Rate Output and Quadrature Compensation in Vibratory MEMS Gyroscopes," *Sensors Journal*, Vol. 7, pp. 1639-1652, 2007.

[4] J. Seeger, A. J. Rastegar, and M. T. Tormey, "Method and apparatus for electronic cancellation of quadrature error," *U.S. Patent* 0 180 908 A1, Aug. 9, 2007.

[5] W. A. Clark and R. T. Howe, "Surface micromachined z-axis vibratory rate gyroscope," *Solid-State Sensor and Actuator Workshop*, Hilton Head Island, SC, June, 1996, pp. 283–287.

[6] S. E. Alper and Tayfun Akin, "A single-crystal silicon symmetrical and decoupled MEMS gyroscope on an insulating substrate," *J. of Microelectromechanical Systems*, Vol. 4, pp. 707-717, 2005.

[7] A. A. Trusov, A.R. Schofield and A.M. Shkel, " Gyroscope architecture with structurally forced anti-phase drive-mode and linearly coupled anti-phase sense-mode," *Solid-State Sensors, Actuators and Microsystems Conference*, Denver, CO, June, 2009, pp. 660-663.

[8] F. Ayazi, "Multi-DOF inertial MEMS - From gaming to dead reckoning," *Solid-State Sensors, Actuators and Microsystems Conference*, Beijing, China, June, 2011, pp. 2805-2808.

[9] J. A. Green, S. J. Sherman, J. F. Chang, and S. R. Lewis," Single-chip surface-micromachined integrated gyroscope with 50/spl deg//hour root Allan variance," *Solid-State Circuits Conference*, San Francisco, CA, USA, February, 2002, pp. 426-427.

[10] A. Sharma, M. F. Zaman, M. Zucher, and F. Ayazi, "A 0.1°/HR bias drift electronically matched tuning fork microgyroscope," *Micro Electro Mechanical Systems Conference*, Tucson, AZ, January, 2008, pp. 6-9.

[11] F.-Y. Lee, K.-C. Liang, Emerson Cheng and W. Fang, "Design and implementation of a fully-decoupled tuning fork (FDTF) MEMS vibratory gyroscope for robustness improvement," *Solid-State Sensors, Actuators and Microsystems Conference*, Anchorage, AK, June, 2015, pp. 1160-1163.

[12] C.-W. Cheng, K.-C. Liang, C.-H. Chu, D. A. Horsley, and W. Fang, "Single chip process for sensors implementation, integration, and condition monitoring," *Solid-State Sensors, Actuators and Microsystems Conference*, Barcelona, June, 2013, pp. 1075-1078.

CONTACT

*W. Fang, tel: +886-3-5742923; fang@pme.nthu.edu.tw